

Cite this: *Chem. Sci.*, 2015, 6, 2782

## *In vitro* and *in vivo* comparative and competitive activity-based protein profiling of GH29 $\alpha$ -L-fucosidases†

Jianbing Jiang,<sup>‡,a</sup> Wouter W. Kallemeijen,<sup>‡,b</sup> Daniel W. Wright,<sup>c</sup> Adrianus M. C. H. van den Nieuwendijk,<sup>a</sup> Veronica Coco Rohde,<sup>a</sup> Elisa Colomina Folch,<sup>a</sup> Hans van den Elst,<sup>a</sup> Bogdan I. Florea,<sup>a</sup> Saskia Scheij,<sup>b</sup> Wilma E. Donker-Koopman,<sup>b</sup> Marri Verhoek,<sup>b</sup> Nan Li,<sup>a</sup> Martin Schürmann,<sup>d</sup> Daniel Mink,<sup>d</sup> Rolf G. Boot,<sup>b</sup> Jeroen D. C. Codée,<sup>a</sup> Gijsbert A. van der Marel,<sup>a</sup> Gideon J. Davies,<sup>c</sup> Johannes M. F. G. Aerts<sup>\*ab</sup> and Herman S. Overkleeft<sup>\*a</sup>

GH29  $\alpha$ -L-fucosidases catalyze the hydrolysis of  $\alpha$ -L-fucosidic linkages. Deficiency in human lysosomal  $\alpha$ -L-fucosidase (FUCA1) leads to the recessively inherited disorder, fucosidosis. Herein we describe the development of fucopyranose-configured cyclophellitol aziridines as activity-based probes (ABPs) for selective *in vitro* and *in vivo* labeling of GH29  $\alpha$ -L-fucosidases from bacteria, mice and man. Crystallographic analysis on bacterial  $\alpha$ -L-fucosidase confirms that the ABPs act by covalent modification of the active site nucleophile. Competitive activity-based protein profiling identified L-fuconojirimycin as the single GH29  $\alpha$ -L-fucosidase inhibitor from eight configurational isomers.

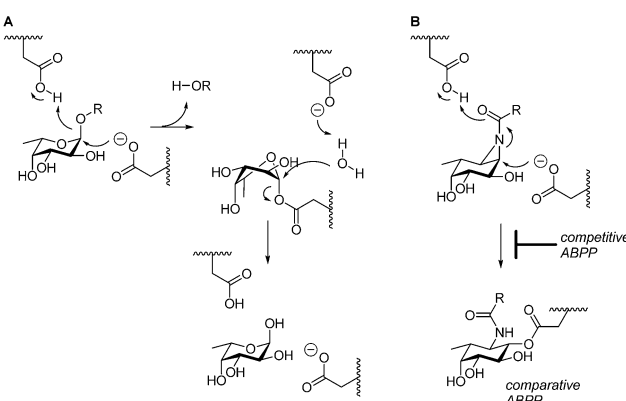
Received 3rd December 2014  
Accepted 9th February 2015

DOI: 10.1039/c4sc03739a  
[www.rsc.org/chemicalscience](http://www.rsc.org/chemicalscience)

## Introduction

GH29  $\alpha$ -L-fucosidases catalyze the hydrolysis of terminal  $\alpha$ -L-fucosidic linkages.<sup>1</sup> The GH29 (ref. 2) glycoside hydrolase family of retaining  $\alpha$ -L-fucosidases contains members from various kingdoms of life including the eukaryota<sup>3</sup> and bacteria (for example, *Bacteroides thetaiotaomicron*,<sup>4</sup> *Sulfolobus solfataricus*,<sup>5</sup> and *Thermotoga maritima*<sup>6</sup>). GH29  $\alpha$ -L-fucosidases process their substrate with overall retention of configuration at the anomeric center of the cleaved fucopyranose and do so through a double-displacement mechanism. In this mechanism, first proposed by Koshland,<sup>7</sup> (Fig. 1A),  $S_N2$  displacement of the aglycon (activated through protonation by the general acid/base residue) by nucleophilic attack of the catalytic nucleophile yields a fucosyl-enzyme intermediate, which is subsequently hydrolyzed to yield  $\alpha$ -L-fucopyranose together with the released aglycon.

Two GH29  $\alpha$ -L-fucosidases are expressed in man. Of these, FUCA1 is found in lysosomes whereas FUCA2 is secreted into the plasma.<sup>8</sup> Deficiency of FUCA1  $\alpha$ -L-fucosidase activity causes fucosidosis,<sup>9</sup> a rare autosomal recessive lysosomal storage disorder. Next to its role in lysosomal turnover of fucosylated substrates, FUCA1 is also involved in sperm transport and sperm–egg interactions.<sup>10</sup> FUCA1 activity levels are considered to be a biomarker for cellular senescence<sup>11</sup> as well as for the diagnosis of hepatocellular cancers.<sup>12</sup> Deficiency of human FUCA2 has been shown to protect against *Helicobacter pylori* adhesion to gastric cancer cells.<sup>8</sup>



<sup>a</sup>Leiden Institute of Chemistry, Leiden University, P. O. Box 9502, 2300 RA Leiden, The Netherlands. E-mail: [h.s.overkleeft@chem.leidenuniv.nl](mailto:h.s.overkleeft@chem.leidenuniv.nl); [j.m.aerts@amc.uva.nl](mailto:j.m.aerts@amc.uva.nl)

<sup>b</sup>Department of Medical Biochemistry, Academic Medical Center, Meibergdreef 15, 1105 AZ Amsterdam, The Netherlands

<sup>c</sup>Department of Chemistry, University of York, Heslington, York, YO10 5DD, UK

<sup>d</sup>DSM Innovative Synthesis, Urmonderbaan 22, NL-6167 RD Geleen, The Netherlands

† Electronic supplementary information (ESI) available: Experimental part including synthesis procedures, characterization data, copies of NMR spectra of new compounds, supporting biological figures and crystallographic information. See DOI: [10.1039/c4sc03739a](https://doi.org/10.1039/c4sc03739a)

‡ These authors contributed equally.

Fig. 1 (A) Double-displacement mechanism of retaining  $\alpha$ -L-fucosidases. (B) Comparative and competitive activity-based profiling of GH29  $\alpha$ -L-fucosidases presented here.



The biological and biomedical relevance of GH29 retaining  $\alpha$ -L-fucosidases warrant the development of efficient methods to monitor their functional state and activity *in vitro*, *in situ* and *in vivo*. In this respect, activity-based probes (ABPs) have shown their merit as tools to detect active enzyme molecules in their native environment (Fig. 1B).<sup>13</sup> We have previously reported the use of cyclophellitol aziridines as scaffolds for the design of *in situ* and *in vivo* active ABPs directed at GH1 retaining  $\beta$ -glucosidases<sup>14</sup> and GH27 retaining  $\alpha$ -galactosidases.<sup>15</sup> The specificity of these probes appeared due to their configuration, with the  $\beta$ -glucopyranose configured cyclitol aziridine being highly selective towards retaining  $\beta$ -glucosidases and their  $\alpha$ -galacto-configured counterparts selective towards  $\alpha$ -galactosidases. Here we describe the development of retaining GH29  $\alpha$ -L-fucosidase ABPs. The ABPs are based on the cyclophellitol aziridine structure having  $\alpha$ -L-fucoside configuration and are equipped with a green (1, JJB256) or red (2, JJB244) BODIPY fluorophore and biotin tag (3, JJB243) (Fig. 2). We reveal that these probes are highly sensitive and selective and can be used for *in situ* and *in vivo* monitoring of mammalian and bacterial GH29 retaining  $\alpha$ -L-fucosidases.

We also demonstrate that ABPs 1 and 2 can be used in a competitive activity-based protein profiling (ABPP) assay<sup>16</sup> to identify rapidly retaining  $\alpha$ -L-fucosidase inhibitors from a library of eight configurational isomers of deoxy-L-fuconojirimycin (6–13); a library we prepared specifically for this purpose. Finally we unambiguously establish the validity of the cyclophellitol aziridine design platform for ABP development of retaining glycosidases by solving the crystal structure of retaining  $\alpha$ -L-fucosidase from *Bacteroides thetaiotaomicron* 2970, covalently bound to *N*-acyl cyclophellitol aziridines 4 and 5.

## Results and discussion

The synthesis of  $\alpha$ -L-fucopyranose-configured cyclophellitol aziridine-based target compounds started with aldol condensation of aldehyde 15 and chiral acrylamide 14, following the procedure reported<sup>17</sup> by Llebaria and co-workers for the enantiomer of 16 (Scheme 1). Reductive removal of the Evans

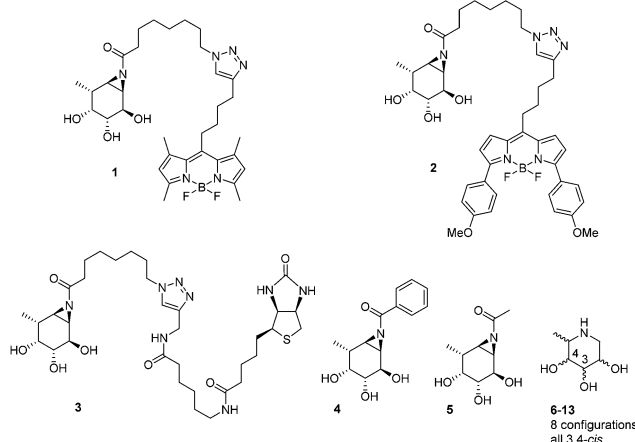
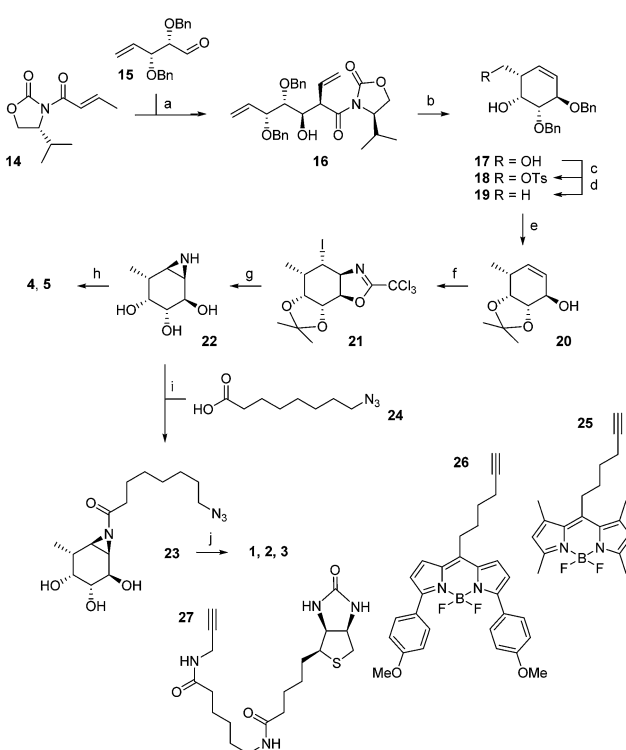


Fig. 2 Structures of inhibitors and ABPs presented in this study.

template in 16 followed by ring-closing metathesis yielded according to the Llebaria procedure<sup>17</sup> partially protected L-galactopyranose-configured cyclohexene 17 in good yield. Tosylation of the primary alcohol in 17 was followed by hydride displacement of the tosylate to afford L-fucopyranose-configured cyclohexene 19. The benzyl groups in 19 were reduced under Birch conditions, after which the *cis*-diol was protected as the isopropylidene acetal to give 20. The secondary alcohol in 20 was transformed into the corresponding trichloroacetimidate after which iodocyclisation yielded in a stereospecific fashion intermediate 21 analogous to the procedure we reported for the synthesis of retaining  $\beta$ -glucosidase ABPs.<sup>18</sup> Acidic hydrolysis of both acetal and iminal in 21 was followed by base-induced intramolecular nucleophilic substitution of the iodine to yield aziridine 22. Acetylation or benzoylation of the aziridine in 22 under the agency of 2-ethoxy-1-ethoxycarbonyl-1,2-dihydroquinoline (EEDQ) following conditions we had developed previously<sup>18</sup> yielded compounds 4 and 5, respectively. EEDQ-induced acylation of 22 with 8-azidoctanoic acid<sup>19</sup> 24 provided azide 23, which was transformed into target ABPs 1, 2 and 3 by conjugation to BODIPY-alkynes 25, 26 and biotin-alkyne 27, respectively, *via* copper(I)-catalyzed Huisgen [2 + 3] cycloaddition. The final compounds were purified by reverse phase HPLC.



Scheme 1 Synthesis of aziridine ABPs 1, 2, 3 and inhibitors 4, 5. Reagents and conditions: (a) DBBT, Et<sub>3</sub>N, CH<sub>2</sub>Cl<sub>2</sub>, -78 °C, 71%; (b) (i) LiBH<sub>4</sub>, THF, 83%; (ii) Grubbs 2<sup>nd</sup> generation, CH<sub>2</sub>Cl<sub>2</sub>, 95%; (c) *p*-TsCl, Et<sub>3</sub>N, CH<sub>2</sub>Cl<sub>2</sub>, 87%; (d) LiAlH<sub>4</sub>, THF, 0 °C to rt, 87%; (e) (i) Li, NH<sub>3</sub> (liq), THF, -60 °C, 73%; (ii) 2,2-dimethoxypropane, CSA, rt, 60%; (f) (i) CCl<sub>3</sub>CN, DBU, CH<sub>2</sub>Cl<sub>2</sub>, rt; (ii) NaHCO<sub>3</sub>, I<sub>2</sub>, H<sub>2</sub>O, rt, 46%; (g) (i) 37% HCl (aq), MeOH, 60 °C; (ii) NaHCO<sub>3</sub>, MeOH, rt, 65%; (h) EEDQ, 24, DMF, 0 °C 25%; (i) EEDQ, 24, DMF, 0 °C 25%; (j) CuSO<sub>4</sub>, sodium ascorbate, 25, 26 or 27, rt, 19% 1, 12% 2, 13% 3.



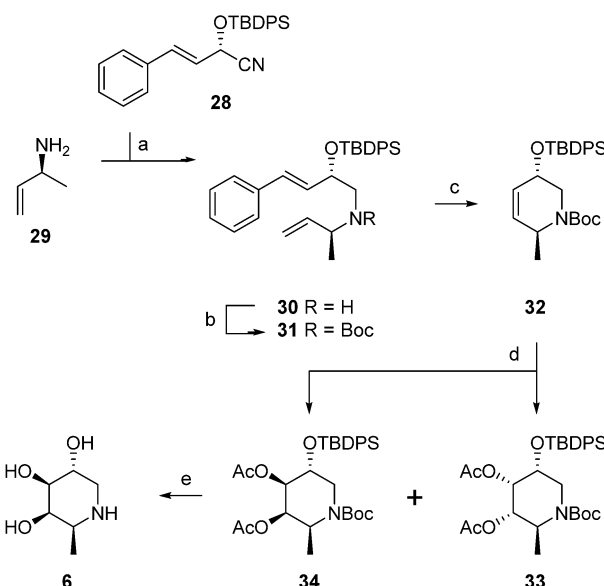
The configurational fuconojirimycin isomers **6–13** (Fig. 3) were synthesized following the strategy exemplified for 1-deoxy-L-fuconojirimycin **6** (Scheme 2). Key steps in the synthetic scheme include a DIBAL-H reduction-transimination-sodium borohydride reduction cascade of reactions involving enantiomerically pure cyanohydrin **28**, prepared employing (*S*)-hydroxynitrile lyase (*S*-HbHNL), from *Hevea brasiliensis* rubber tree,<sup>20</sup> and the allylic amine **29** prepared by reported strategy,<sup>21</sup> to give secondary amine **30**. *N*-Boc protection (**30** to **31**), ring-closing metathesis (**31** to **32**) and Upjohn dihydroxylation afforded a mixture of *syn*-diols, which were acetylated and separated by silica gel purification to yield diastereomers **33** and **34** in a 1 : 3 ratio.

Global deprotection of **34** afforded 1-deoxy-L-fuconojirimycin **6**, the analytical and spectroscopic data of which were in full agreement with those reported in the literature.<sup>22</sup> The seven configurational isomers **7–13** were prepared by alteration of the building blocks and/or the chemical transformations. It should be noted that four out of the eight isomers of fuconojirimycin are derived from **28**. To enable the synthesis of the four enantiomers we needed access to the enantiomer of cyanohydrin **28**, which we prepared using almond (*R*)-hydroxynitrile lyase (*R*-PaHNL).<sup>23</sup>

### In vitro GH29 $\alpha$ -L-fucosidase activity assays

Having the cyclophellitol aziridine inhibitors and probes in hand, we determined their inhibitory potency towards the human lysosomal  $\alpha$ -L-fucosidase, FUCA1. Inhibition potency was determined by measuring the residual enzyme activity using the fluorogenic substrate 4-methylumbelliferyl- $\alpha$ -L-fucopyranoside after pre-incubation of lysates of COS-7 cells over-expressing recombinant human FUCA1, with varying concentrations of the non-fluorescent, irreversible cyclophellitol aziridine inhibitors **4**, **5** and **23**; the ABPs **1** (JJB256), **2** (JJB244), **3** (JJB243), 1-deoxy-L-fuconojirimycin **6**, and the seven fuconojirimycin isomers **7–13**. All *N*-acyl aziridines inhibited human FUCA1 activity with nanomolar  $IC_{50}$  activities (Table 1).

Perusal of the inhibitory data does reveal some trends that allow us to draw some tentative conclusions. *N*-Benzoyl aziridine **4**, bearing a bulky aromatic *N*-benzoate group, is about eight-fold less active compared to its *N*-acetylated counterpart, **5**. In contrast, comparing **5** with **23** reveals that a bulky aliphatic



**Scheme 2** Synthesis of 1-deoxy-L-fuconojirimycin **6**. Reagents and conditions: (a) (i)  $Et_2O$ , DIBAL-H,  $-80\text{ }^\circ C$ , (ii)  $MeOH$ ,  $-90\text{ }^\circ C$ , (iii) amine **29**,  $NaOMe$ , (iv)  $NaBH_4$ ,  $-15\text{ }^\circ C$  to rt, 88%; (b)  $Boc_2O$ ,  $50\text{ }^\circ C$ , 100%; (c) Grubbs 1<sup>st</sup> generation,  $CH_2Cl_2$ , 88%; (d) (i)  $K_2OSO_4 \cdot 2H_2O$ ,  $NMO$ , acetone- $H_2O$  (1 : 1),  $-10\text{ }^\circ C$ , (ii)  $Ac_2O$ , pyridine, DMAP,  $0\text{ }^\circ C$ , 88% (**33** : **34** = 1 : 3); (e) (i)  $K_2CO_3$ ,  $MeOH$ , (ii)  $TBAF$ ,  $THF$ , (iii) 6 M  $HCl$ ,  $MeOH$ , 71%.

*N*-acyl substituent is in fact favored for enzyme inhibition (5-fold increase, Table 1). ABPs **1** and **2**, bearing a BODIPY fluorophore attached to the alkyl chain, inhibit FUCA1 in the same order as their azide precursor **23**. *In situ* inhibition of FUCA1 in living fibroblasts by ABP **1** and **2** occurs with similar efficacy as **23** and ABP **3**, the latter carrying a biotin attached to the alkyl chain. Exposure of cells to ABP **3** revealed in a 25-fold decreased inhibitory potency, suggesting a reduced ability to penetrate into cells to reach the lysosomal FUCA1. The known competitive

**Table 1** *In vitro* and *in situ* inhibition of recombinant human GH29  $\alpha$ -L-fucosidase, given as half-maximal inhibitory concentration ( $IC_{50}$ )<sup>a</sup>

	<i>In vitro</i> $IC_{50}$	<i>In situ</i> $IC_{50}$
<b>Aziridine</b>		
<b>1</b> (JJB256)	$6.9 \pm 0.8$	$28.9 \pm 4.4$
<b>2</b> (JJB244)	$8.7 \pm 1.2$	$157.8 \pm 22$
<b>3</b> (JJB243)	$7.2 \pm 1.1$	$25\,512 \pm 2278$
<b>4</b>	$371.6 \pm 21.2$	$515.4 \pm 72.9$
<b>5</b>	$46.8 \pm 3.4$	$77.9 \pm 9.1$
<b>23</b>	$8.7 \pm 1.1$	$65.4 \pm 7.5$
<b>Iminosugars</b>		
<b>6</b>	$3979 \pm 257$	ND
<b>7–13</b>	$>100\,000$	ND

<sup>a</sup> Values are given in nanomolar. ND: not determined. It should be noted that  $IC_{50}$  values on competitive inhibitors do not compare well to those obtained for mechanism-based inhibitors. The values given above allow for a comparison of inhibitory potency within the two classes of compounds studied.

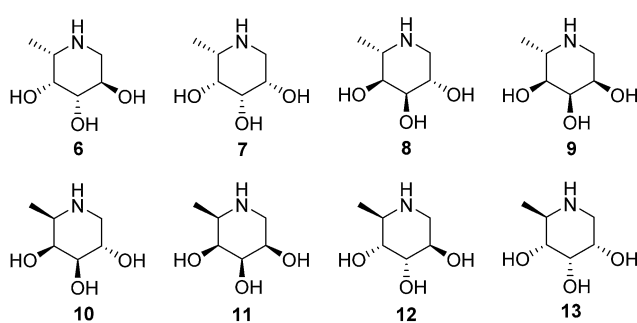


**Fig. 3** Structures of 1-deoxy-L-fuconojirimycin **6** and configurational isomers **7–13**.



fucosidase inhibitor, 1-deoxy-*L*-fuconojirimycin **6** inhibits FUCA1 with an  $IC_{50}$  of 3.9  $\mu$ M, in accordance with the literature values.<sup>24</sup> The seven configurational isomers **7–13** do not significantly inhibit FUCA1 activity up to 100  $\mu$ M, a result that corroborates previous findings on some of the configurational analogues, which were reported as poor fucosidase inhibitors.<sup>25</sup>

As the next research objective, we examined activity-based profiling of GH29  $\alpha$ -L-fucosidases from varying sources with green-fluorescent aziridine ABP **1**, in the presence or absence of excess concentrations of, either the mechanism-based inhibitor **4** or the competitive inhibitor **6**. As is shown in Fig. 4A, ABP **1** efficiently labels purified  $\alpha$ -L-fucosidase from *Bacteroides thetaiotaomicron*. In lysates from an *E. coli* culture overexpressing recombinant  $\alpha$ -L-fucosidase from *Bacteroides thetaiotaomicron* gene 2970, several fluorescent protein bands are visible upon labeling with **1** (ESI Fig. S1†), with the most prominent band at around 50 kDa, corresponding to the predicted molecular weight of the enzyme. Labeling of the major band at 50 kD could moreover be blocked following pre-incubation with either 100  $\mu$ M **4** or with 5 mM **6** (ESI Fig. S1†). Red fluorescent ABP **2** labels  $\alpha$ -(1-2,3,4) and  $\alpha$ -(1-6)-

fucosidases from various bacterial sources in a similar fashion (Fig. 4B).

Subsequently, we exposed lysates of spleens from a healthy human individual and a patient suffering from Gaucher disease to ABP **1**. As can be seen in Fig. 4C, a single fluorescent protein migrating slightly below 50 kDa was fluorescently labeled. The labeled band from human Gaucher spleen lysate is considerably more intense than the corresponding band in healthy human spleen, reflecting elevated  $\alpha$ -L-fucosidase activity in the former. This result corroborates earlier observations that mRNA encoding lysosomal glycosidases are upregulated in Gaucher tissue.<sup>26</sup> As before, labeling with ABP **1** was suppressed after pre-treatment with either *N*-benzoyl aziridine **4** or *L*-fuconojirimycin **6**. To further ascertain that ABP **2** labels mammalian GH29 retaining  $\alpha$ -L-fucosidases we performed a number of control experiments (ESI Fig. S2a†). Compound **1** labeled both FUCA1 and FUCA2 that were overexpressed in COS cells. Treatment of murine spleen lysates with **1** yielded a result essentially as observed for healthy human tissue (ESI Fig. S2b†).

Finally, we evaluated the simultaneous labeling of retaining  $\beta$ -glucosidases and retaining  $\alpha$ -L-fucosidase. To this end we incubated tissue lysates with **1** and our previously<sup>18</sup> reported broad-spectrum activity-based retaining  $\beta$ -glucosidase probe, JJB75 (see for its structure, ESI Fig. S3†). As can be seen (Fig. 4D) the applied ABPs label a distinct set of proteins. Since they bear complementary fluorophores they can be used jointly to profile both retaining glycosidase families in a single experiment.

The FUCA1 enzymatic activity is maximal at around pH 4.5 (see ESI Fig. S4†), consistent with the acidic pH of its natural lysosomal environment. Labeling efficiency with **1** largely reflects the pH dependence of FUCA1 at pH below 7. Of note, the pH dependence of labeling of FUCA1 does not follow that of its enzymatic activity. At alkaline conditions, where enzymatic activity is low, labeling still proceeds. We made similar observations in the past for ABPP of retaining  $\beta$ -exoglucosidases using cyclophellitol  $\beta$ -aziridine ABPs.<sup>14</sup> This result reveals the high reactivity of the aziridine probes in the initial displacement step employed by retaining glycosidases, a feature which, in conjunction with their selectivity in binding and relative stability in physiological environment, explains their efficacy as activity-based glycosidase probes.<sup>27</sup>

Assessment of fluorescent labeling kinetics by employing 10 nM **1** labeling at stoichiometric concentrations of rhFUCA1 at 4 °C and 37 °C revealed that, during time-course experiments, examined on SDS-PAGE gels, labeling is near complete within the first minute at 4 °C (ESI Fig. S5a†), impairing accurate determination of kinetic constants. This rapid reaction with both **1** and **2** also precluded a classic determination of kinetic constants following a time-dependent decrease in detectable 4-methylumbelliflone (ESI Fig. S5b†).

#### In vivo GH29 $\alpha$ -L-fucosidase assays

The ability of **1** to label  $\alpha$ -L-fucosidase in living mice was investigated next. Four wild-type C57Bl/6J male mice were injected with 100  $\mu$ L vehicle (PBS) or PBS containing 10, 100 or 1000 pmol **1**. After two hours, the mice were anesthetized,

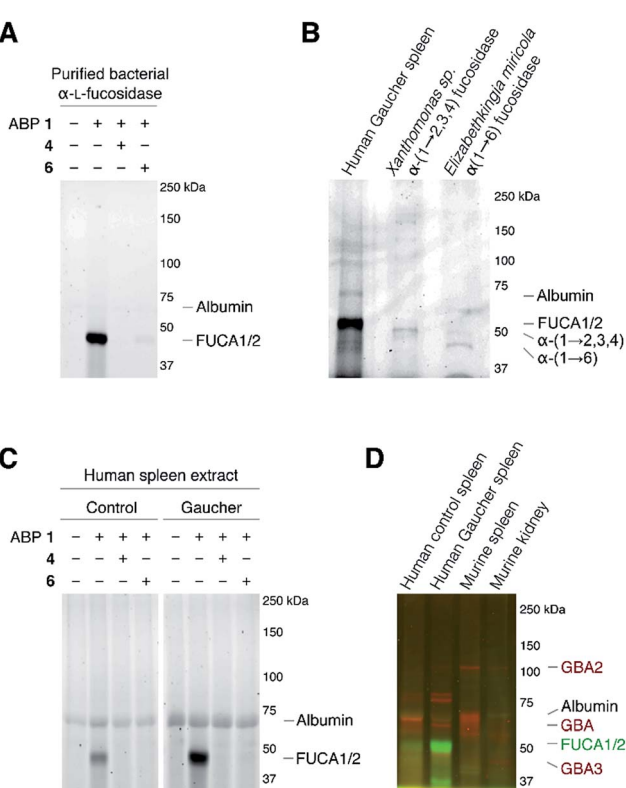


Fig. 4 *In vitro* activity-based protein profiling of GH29  $\alpha$ -L-fucosidases. (A) Labeling with ABP **1** of recombinant  $\alpha$ -L-fucosidase from *Bacteroides thetaiotaomicron* 2970. (B) *In vitro* labeling of lysate of spleen from a Gaucher disease patient,  $\alpha$ -(1-2,3,4)-fucosidase from *Xanthomonas* sp. and  $\alpha$ -(1-6)-fucosidase from *Elizabethkingia miricola* with ABP **2**. (C) *In vitro* labeling of human healthy and Gaucher disease spleen. (D) Direct labeling of GH29  $\alpha$ -L-fucosidases with green-fluorescent ABP **1** and retaining  $\beta$ -glucosidases GBA, GBA2 and GBA3 with red-fluorescent JJB75.<sup>18</sup> The location of albumin auto-fluorescence is designated on each gel.



perfused with PBS and then brain, spleen, liver and kidney tissues were isolated. Tissue homogenates were prepared and each lysate was labeled prior to gel electrophoresis with red-fluorescent cyclophellitol  $\beta$ -aziridine JJB75, which labels  $\beta$ -exoglycosidases as loading control (ESI Fig. S6†). Furthermore, tissue homogenates of vehicle-treated animals were labeled with excess **1** to visualize the maximal  $\alpha$ -L-fucosidase labeling achievable in each tissue.

After treatment of mice with **ABP 1**, a dose-dependent labeling of retaining  $\alpha$ -L-fucosidases is observed in spleen, liver and kidney (Fig. 5). Injection of 1000 pmol **1** results in substantial labeling of  $\alpha$ -fucosidase in spleen, liver and kidney. Detected fluorescence levels are comparable to that in matching samples from vehicle-treated mice incubated *in vitro* with excess **1**. In contrast, no *in vivo* brain FUCA1 labeling was observed after any of the administered doses of **ABP 1**, and we conclude that **ABP 1**, just as its  $\beta$ -glucose and  $\alpha$ -galactose congeners,<sup>14,15</sup> does not penetrate the brain.

#### Competitive activity-based GH29 $\alpha$ -L-fucosidase profiling

Having established the efficacy of **ABP 2** to selectively label GH29 retaining  $\alpha$ -L-fucosidases from various sources in an activity-based manner, we determined the inhibition potential of deoxyfuconojirimycin **6** and its 7 stereoisomers **7–13** in a competitive ABPP format (Fig. 6). In contrast to **6**, none of the seven configurational isomers **7–13** were capable of blocking **ABP 1** labeling of  $\alpha$ -L-fucosidase, a result that matches with the data on inhibition of recombinant FUCA1 in the fluorogenic activity assay (Table 1).

#### Identification of biotin labeled GH29 $\alpha$ -L-fucosidases

To further determine the specificity of the developed ABPs, we have analyzed the ABP-labeled proteins in a complex tissue homogenate. For this purpose, we incubated Gaucher spleen lysate with biotinylated **ABP 3** or with DMSO only (control) or competitive **ABP 3**-labeling by first incubating with fluorescent **ABP 1**. Glycosylated proteins were then enriched *via* ConA, followed by affinity purification with streptavidin coated paramagnetic beads. The identity of biotinylated and **ABP 3**-labeled proteins was determined by on-bead digestion with trypsin,

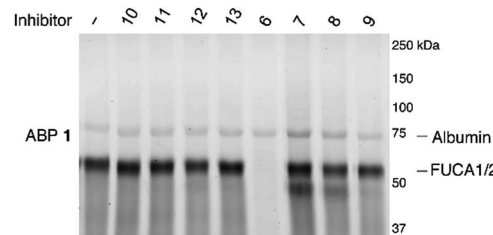


Fig. 6 Competitive ABPP on recombinant FUCA1 with deoxyfuconojirimycin **6** and configurational analogues **7–13** towards  $\alpha$ -L-fucosidases, with **ABP 1** labeling as readout.

peptide analysis by LC-MS/MS and matching against the human UniProt database, using the Mascot search engine as previously reported.<sup>14</sup> FUCA1 was identified after **ABP 3** pull-down as one of the top identified proteins (Table S1A) in the ESI data, but was not found in the competitive (Table S1B) or untreated control (Table S1C†). Proteins with higher scores were background proteins such as abundant endogenously biotinylated PCCA and PC, and keratin contaminations. FUCA1 was selectively found in the **ABP 3**-pull down experiment only. ESI Table S2† shows the analysis parameters of the identified peptides from FUCA1, with accuracy below 5 ppm, and Mascot ion scores above 40 (indicating reliable MS/MS fragment annotation and match) and manually curated fragmentation patterns. These results show FUCA1 can be undisputedly affinity purified and identified *via* biotinylated **ABP 3**. Moreover the binding of **ABP 3** can be completely blocked by pre-incubation with **ABP 1**, which may indicate that both ABPs bind at the same site of the enzyme.

#### 3-D crystal structure analysis of bacterial FUCA1 complexed to 4 and 5

In order to obtain experimental evidence for the formation of a covalent adduct between  $\alpha$ -L-fucosidase and ABPs **1**, **2** and **3**, a crystal structure of *BtFuc2970* (often used as a surrogate for the mammalian enzyme) with mechanism-based inhibitor **4** was obtained (PDB code 4WSK). While the resulting crystal structure clearly demonstrates the formation of an enzyme–**4** complex, electron density around the aryl group of the inhibitor “aglycon” moiety was close to the side-chain of the catalytic acid/base of the enzyme, residue E288 (ESI Fig. S7†) resulting in disorder. This likely reflects steric clashing and considerable conformational flexibility in the **4** aglycon when bound to *BtFuc2970*. “Aglycon” here reflects the aziridine *N*-acyl moiety to which the BODIPY tags are grafted in ABPs **1** and **2** and which is designed to occupy the space normally occupied by the substrate fucoside.

In our design of aziridine-based retaining *exo*-glycosidase ABPs we made the assumption that such aglycon-like moieties would not interfere with enzyme binding (this also based on the numerous fluorogenic substrates that are in use to study exoglycosidases and in which the aglycon moiety can take on made shapes and sizes). The 3-D fold of *BtFuc2970*, however, appears not to provide sufficient space to accommodate an extended aryl

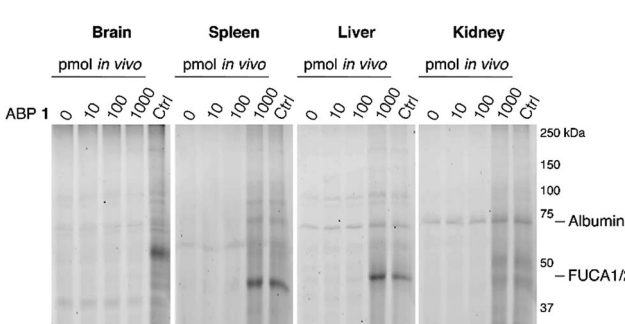


Fig. 5 *In vivo* labeling of  $\alpha$ -L-fucosidases in mice with various concentrations of **ABP 1** during 2 hours. *In vivo* labeling compared to maximal labeling with excess **ABP 1** of matched homogenates (Ctrl). The location of albumin autofluorescence is designated on each gel.



aglycon pendant to the atom, which would equate to the ring oxygen in fucose. In order to minimize steric clashes, *BtFuc2970* was subsequently incubated with **5**. The crystal structure of the resulting complex (PDB code 4WSJ) revealed unambiguous electron density for the presence of a covalent enzyme–5 complex (Fig. 7). The complex has C–O bond lengths between the *BtFuc2970* catalytic nucleophile and **5** of *ca.* 1.43 Å as would be expected for a C–O ester bond. As expected from the reduction in aglycon size, **5** is better ordered than **4** when bound to the bacterial enzyme and provides a clearer definition of the resulting conformation and interactions. Upon *trans*-dixial opening of the acylaziridine the covalently bound and substituted cyclohexane adopts a slightly distorted  $^3\text{H}_4$  conformation (between  $^3\text{H}_4$  and  $^3\text{S}_1$ ); consistent with the expected catalytic itinerary.<sup>28</sup>

## Conclusions

We have developed the potent and selective aziridine-based ABPs **1**, **2** and **3** for selective profiling of active GH29  $\alpha$ -L-fucosidases in cell extracts from bacteria, mice and man as well as *in vivo* in mice. Labeling of GH29 retaining  $\alpha$ -L-fucosidases with our L-fucopyranose-configured, cyclophellitol aziridine-based ABPs proceeds with good efficiency and high selectivity both *in vitro* and *in vivo* with the single caveat that the probes do not penetrate brain tissue in mice. The covalent irreversible aziridine inhibitors proved much more potent than their imino-sugar counterparts, of which L-fuconojirimycin **6** appeared to be the single compound from this set of configurational isomers that is able to inhibit FUCA1 in a competitive ABPP setting. The crystal structures of  $\alpha$ -L-fucosidase from *Bacteroides thetaiotaomicron* in complex with compound **4** and **5** provide strong evidence for the covalent binding of cyclophellitol aziridine to active  $\alpha$ -L-fucosidases and by this virtue the validity of the cyclophellitol aziridine design for activity-based profiling of retaining glycosidases that employ the Koshland double displacement mechanism. Whereas aziridines and epoxides

that are annulated to cyclohexane rings preferably open in a *trans*-dixial fashion through a chair-like transition state, reaction with the  $\alpha$ -L-fucosidase nucleophile takes place at the aziridine carbon corresponding to the anomeric center of a substrate  $\alpha$ -L-fucoside. This corresponds to ring opening to yield a skew boat, as is observed in the trapped enzyme active site in the co-crystal.

In conclusion, we offer ABPs **1**, **2** and **3** as reagents for the discovery and annotation of new members of the GH29 family of  $\alpha$ -L-fucosidase in comparative ABPP experiments, for monitoring retaining  $\alpha$ -L-fucosidase activities in health and disease, and for the discovery of inhibitors able to interfere with specific  $\alpha$ -L-fucosidases in competitive ABPP experiments. ABPs **1**, **2** and **3** add to our growing series of *in situ* and *in vivo* active retaining glycosidase ABPs and moreover their design hold promise for the design of ABPs targeting retaining glycosidases recognizing and processing differently configured and substituted carbohydrates.

## Experimental section

### Synthesis

The synthesis, analytical and spectroscopical analysis of L-fuconojirimycin configured cyclophellitol aziridines **1**–**5** and L-fuconojirimycin isomers **6**–**13** is described in the ESI.<sup>†</sup>

### Biological assays

**Materials.** Cyclophellitol  $\beta$ -aziridine ABP JJB75 was synthesized as described earlier.<sup>18</sup> Gaucher patients were diagnosed on the basis of reduced GBA activity and demonstration of an abnormal genotype.<sup>30</sup> Cell lines were cultured in HAMF12-DMEM medium (Invitrogen) supplied with 10% (v/v). Spleens from a normal subject and a patient suffering from type 1 Gaucher were collected after splenectomy and immediately stored frozen.

**Molecular cloning and recombinant expression.** The coding sequences of *H. sapiens* FUCA1 (NCBI reference sequence XM\_005245821.1, using forward primer 5'-GGGGACAAGTTG TACAAAAAAAGCAGGCTCCACCACCATGGGGCTCGGGGATG-3' and reverse primer 5'-GGGGACCACTTGTACAAGAAAGCTGGG TCTTACTTCACTCCTGTAGCTTAT-3'), and of *H. sapiens* FUCA2 (NCBI reference sequence NM\_032020.4, using forward primer 5'-GGGGACAAGTTGTACAAAAAGCAGGCTC CACCA CATGGGGCCCAGGAGCTC-3' and reverse primer 5'-GGGGAC CACTTGTACAAGAAAGCTGGGTCT TAGATCACATTAGTCAGG GCTA-3') were amplified *via* PCR and cloned into pDNOR-221 and thereafter sub-cloned in pcDNA<sup>TM</sup>-DEST40 vector using the Gateway system (Invitrogen). Correctness of all constructs was verified by sequencing. Confluent COS-7 cells were transfected with pcDNA3.1 empty vector (Mock) or the vector with described insert in conjunction with FuGENE (Roche). After 72 hours, medium isolated and frozen at  $-80$  °C and cells were harvested by scraping in 25 mM potassium phosphate buffer (pH 6.5, supplemented with 0.1% (v/v) Triton X-100 and protease inhibitor cocktail (Roche)). After determination of the protein

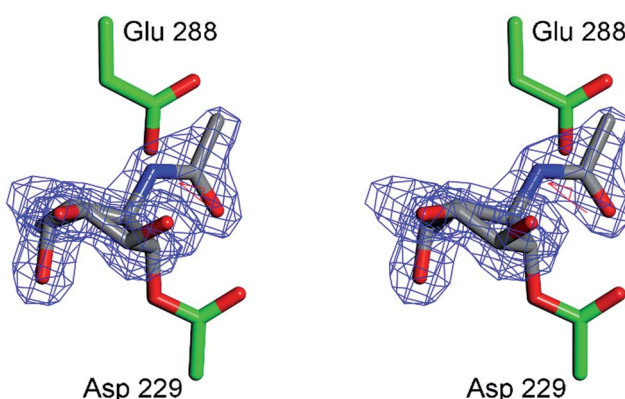


Fig. 7 Crystal structure of  $\alpha$ -L-fucosidase from *Bacteroides thetaiotaomicron* in complex with **5**. Catalytic residues are annotated: Asp 229 (nucleophile) and Glu 288 (acid/base). Electron density displayed is  $F_o - F_c$  density from phases calculated prior to the inclusion of **5** in refinement, contoured at  $3\sigma$ . Figure was prepared using CCP4MG.<sup>29</sup>



concentration (BCA kit, Pierce), lysates were aliquoted and frozen at  $-80^{\circ}\text{C}$ .

**Enzyme activity assays.** The enzymatic activity of  $\alpha$ -L-fucosidase was assayed at  $37^{\circ}\text{C}$  by incubating with 1.5 mM 4-methylumbelliferyl- $\alpha$ -L-fucopyranoside as substrate in 150 mM McIlvaine buffer, pH 4.5, supplemented with 0.1% (w/v) BSA. To determine the apparent  $IC_{50}$  value, COS-7 cell lysate containing over-expressed human recombinant FUCA1 was pre-incubated with a range of inhibitor dilutions for 30 min at  $37^{\circ}\text{C}$ . The reaction was quenched by adding excess NaOH-glycine (pH 10.6), after which fluorescence was measured with a fluorimeter LS55 (Perkin Elmer) using  $\lambda_{\text{EX}}$  366 nm and  $\lambda_{\text{EM}}$  445 nm.

**In vitro labeling and SDS-PAGE analysis.** All pre-incubations and ABP labeling-reactions occurred for 30 min at  $37^{\circ}\text{C}$ . Total lysates (50  $\mu\text{g}$ ), medium (500  $\mu\text{g}$ ) or purified protein preparations (5  $\mu\text{g}$ ) were labeled with 1  $\mu\text{M}$  JJB256 1 or JJB244 2, dissolved in 150 mM McIlvaine buffer, pH 4.5, incubating for 30 min at  $37^{\circ}\text{C}$ . For ABPP, protein preparations were pre-incubated with compounds 4 (100  $\mu\text{M}$ ), 6 (100  $\mu\text{M}$ ), 7–13 (1 or 5 mM, specified in the main text) prior to the addition of 100 nM fluorescent ABPs. Influence of pH on ABP labeling involved pre-incubation at pH 3–10 prior to addition of 100 nM ABP 1. Direct labeling of retaining  $\beta$ -glucosidases occurred at pH 5.0 in conjunction with 100 nM ABP JJB75. Samples were then denatured with 5  $\times$  Laemmli buffer (50% (v/v) 1 M Tris-HCl, pH 6.8, 50% (v/v) 100% glycerol, 10% (w/v) DTT, 10% (w/v) SDS, 0.01% (w/v) bromophenol blue), boiled for 4 min at  $100^{\circ}\text{C}$ , and separated by gel electrophoresis on 10% (w/v) SDS-PAGE gels running continuously at 90 V.<sup>13,14</sup> Wet slab-gels were scanned on fluorescence using a Typhoon Variable Mode Imager (Amersham Biosciences) using  $\lambda_{\text{EX}}$  488 nm and  $\lambda_{\text{EM}}$  520 nm (band pass filter 40 nm) for green fluorescent JJB256 1 and  $\lambda_{\text{EX}}$  532 nm and  $\lambda_{\text{EM}}$  610 nM (band pass filter 30 nm) for red fluorescent JJB244 2 and JJB75.

**In vivo labeling.** The appropriate ethics committee for animal experiments approved all experimental procedures. Wild-type C57Bl/6J male mice were obtained from Harlan and fed a commercially available lab diet (RMH-B; Hope Farms). Four C57BL/6J mice were injected intraperitoneally with 100  $\mu\text{L}$  sterile PBS (vehicle) or PBS containing 10, 100, or 1000 pmol of ABP 1 (about 0.2  $\mu\text{g kg}^{-1}$ , 2  $\mu\text{g kg}^{-1}$ , and 20  $\mu\text{g kg}^{-1}$ , respectively). At 2 h post-administration, urine was collected and the mice were anesthetized with FFM mix (25/25/50 fentanylcitrate/midazalam/H<sub>2</sub>O), blood was collected and perfused with PBS at 3.0 mL min<sup>-1</sup>. Then urine and organs were collected and directly frozen in liquid nitrogen. Homogenates were made in 25 mM potassium phosphate buffer, pH 6.5, supplemented with 0.1% (v/v) Triton X-100 and protease inhibitor cocktail (Roche). After determination of protein concentration (BCA kit, Pierce), 50  $\mu\text{g}$  total protein was incubated with 100 nM red fluorescent JJB75 and analyzed by SDS-PAGE. As controls, matching tissue homogenates of vehicle-treated animals were concomitantly labeled with 1  $\mu\text{M}$  ABP 1 and 100 nM JJB75 prior to SDS-PAGE.

**ABP pulldown and LC-MS/MS analysis.** Gaucher spleen lysate (1 g) was cut with a sterile scalpel, mixed with 4 mL 25 mM potassium phosphate buffer (pH 6.5, supplemented with 0.1% (v/v) Triton X-100 and protease inhibitor cocktail (Roche)) and

sonicated three times for 10 seconds at 100% strength and kept on ice. After 2 min, procedure repeated twice. Lysate was then centrifuged for 10 min at 10 000 g, supernatant collected carefully, protein concentration determined and 200 mg total protein was then incubated with either 0.1% (v/v) DMSO, ABP 1 or ABP 3, or firstly with 10  $\mu\text{M}$  ABP 1 followed by 10  $\mu\text{M}$  of ABP 3, each step taking 30 min at  $37^{\circ}\text{C}$ , in a total volume of 1 mL McIlvaine buffer, pH 4.5. Glycosylated biomolecules were enriched by using 1 mL ConA-Sepharose per sample, according to manufacturer's instructions (Amersham Pharmacia Biotech AB, Sweden) and subsequently denatured by the presence of 2% (w/v) SDS and boiling for 5 min at  $100^{\circ}\text{C}$ . From here on, samples were prepared for MS as published earlier.<sup>14</sup> After desalting on StageTips, peptides were analyzed with a 2 h gradient of 5–25% ACN on nano-LC, hyphenated to an LTQ-Orbitrap and identified via the Mascot protein search engine.<sup>14</sup>

**X-ray crystallography.** Recombinant *Bacteroides thetaiotaomicron* 2970  $\alpha$ -L-fucosidase (*BtFuc2970*) was prepared as described previously.<sup>28</sup> Protein crystals were obtained through hanging (Crystals soaked with compound 5) or sitting (crystals soaked with compound 4) drop vapor diffusion (for further details see PDB file headers). Compounds 4 and 5 were dissolved in crystallization mother liquor at a concentration of 5 or 20 mM respectively and added to crystallization drops containing crystals of *BtFuc2970* in a 1 : 1 ratio. After ca. 1 h soaking with ligands, crystals were fished into cryo-protectant solutions (mother liquor supplemented with 20% v/v glycerol) and cryo-cooled in liquid nitrogen. Diffraction data were collected at Diamond Light Source. Diffraction images were indexed and integrated using MOSFLM<sup>29</sup> (4) or XDS<sup>31</sup> (5) and scaled and merged using AIMLESS.<sup>32</sup> Crystals grew in an almost isomorphous space group to PDB entry 4JFV, and coordinates from this entry were used directly to obtain a starting model for refinement. Iterative stages of model-building (COOT<sup>33</sup>) and maximum-likelihood refinement (REFMAC5 (ref. 34)) were conducted to yield final models. Maximum-likelihood restraints for compounds 4 and 5 were created using the PRODRG online server<sup>35</sup> and link restraints generated using JLIGAND.<sup>36</sup> X-ray crystallographic data statistics are available in ESI Table S3.†

## Acknowledgements

The work in Leiden and Amsterdam was supported by the China Research Council (PhD grant, to JBJ), the Netherlands Organization for Scientific Research (NWO, ChemThem grant to JMA and HSO) and the European Research Council (ERC AdG 'ChemBioSphing', to HSO and JMA). The work in York was supported by the Biotechnology and Biological Sciences Research Council (BBSRC) through a Ph.D. studentship to D. W. W. ABPP work in York is further supported through the ERC (ERC-2012-AdG-322942). The authors thank ChemAxon for the academic licensed software.

## Notes and references

- 1 J. Intra, M.-E. Perotti, G. Pavesi and D. Horner, *Gene*, 2007, 392, 34–46.



2 V. Lombard, H. Golaconda Ramulu, E. Drula, P. M. Coutinho and B. Henrissat, *Nucleic Acids Res.*, 2014, **42**, D490–D495.

3 S. W. Liu, C. S. Chen, S. S. Chang, K. K. T. Mong, C. H. Lin, C. W. Chang, C. Y. Tang and Y. K. Li, *Biochemistry*, 2009, **48**, 110–120.

4 L. Guillotin, P. Lafite and R. Daniellou, *Biochemistry*, 2014, **53**, 1447–1455.

5 B. Cobucci-Ponzano, M. Mazzzone, M. Rossi and M. Moracci, *Biochemistry*, 2005, **44**, 6331–6342.

6 F. A. Shaikh, A. L. van Bueren, G. J. Davies and S. G. Withers, *Biochemistry*, 2013, **52**, 5857–5864.

7 D. E. Koshland, *Biol. Rev.*, 1953, **28**, 416–436.

8 T. W. Liu, C. W. Ho, H. H. Huang, S. M. Chang, S. D. Popat, Y. T. Wang, M. S. Wu, Y. J. Chen and C. H. Lin, *Proc. Natl. Acad. Sci. U. S. A.*, 2009, **106**, 14581–14586.

9 J. S. O'Brien, P. J. Willems, H. Fukushima, J. R. de Wet, J. K. Darby, R. D. Cioccio, M. L. Fowler and T. B. Shows, *Enzyme*, 1987, **38**, 45–53.

10 K. Phopin, W. Nimalamool, L. J. Lowe-Krentz, E. W. Douglass, J. N. Taroni and B. S. Bean, *Mol. Reprod. Dev.*, 2013, **80**, 273–285.

11 D. G. Hildebrand, S. Lehle, A. Borst, S. Haferkamp, F. Essmann and K. Schulze-Osthoff, *Cell Cycle*, 2013, **12**, 1922–1927.

12 M. G. Giardina, M. Matarazzo, R. Morante, A. Lucariello, A. Varriale, V. Guardasole and G. De Marco, *Cancer*, 1998, **83**, 2468–2474.

13 B. F. Cravatt, A. T. Wright and J. W. Kozarich, *Annu. Rev. Biochem.*, 2008, **77**, 383–414.

14 W. W. Kallemeijn, K. Y. Li, M. D. Witte, A. R. Marques, J. Aten, S. Scheij, J. Jiang, L. I. Willems, T. M. Voorn-Brouwer, C. P. van Roomen, R. Ottenhoff, R. G. Boot, H. van den Elst, M. T. Walvoort, B. I. Florea, J. D. Codée, G. A. van der Marel, J. M. Aerts and H. S. Overkleef, *Angew. Chem., Int. Ed. Engl.*, 2012, **51**, 12529–12533.

15 L. I. Willems, T. J. M. Beenakker, B. Murray, S. Scheij, W. W. Kallemeijn, R. G. Boot, M. Verhoek, W. E. Donker-Koopman, M. J. Ferraz, E. R. van Rijssel, B. I. Florea, J. D. C. Codée, G. A. van der Marel, J. M. F. G. Aerts and H. S. Overkleef, *J. Am. Chem. Soc.*, 2014, **136**, 11622–11625.

16 M. J. Niphakis and B. F. Cravatt, *Annu. Rev. Biochem.*, 2014, **83**, 341–377.

17 Y. Harrak, C. M. Barra, A. Delgado, A. R. Castano and A. Llebaria, *J. Am. Chem. Soc.*, 2011, **133**, 12079–12084.

18 K.-Y. Li, J. Jiang, M. D. Witte, W. W. Kallemeijn, H. van den Elst, C.-S. Wong, S. D. Chander, S. Hoogendoorn, T. J. M. Beenakker, J. D. C. Codée, J. M. F. G. Aerts, G. A. van der Marel and H. S. Overkleef, *Eur. J. Org. Chem.*, 2014, **2014**, 6030–6043.

19 O. David, W. J. N. Meester, H. Bieräugel, H. E. Schoemaker, H. Hiemstra and J. H. van Maarseveen, *Angew. Chem., Int. Ed.*, 2003, **42**, 4373–4375.

20 H. Griengl, N. Klempier, P. Pöchlauer, M. Schmidt, N. Shi and A. A. Zabelinskaja-Mackova, *Tetrahedron*, 1998, **54**, 14477–14486.

21 A. D. Campbell, T. M. Raynham and R. J. K. Taylor, *Synthesis*, 1998, 1707–1709.

22 G. W. J. Fleet, A. N. Shaw, S. V. Evans and L. E. Fellows, *J. Chem. Soc., Chem. Commun.*, 1985, 841–842.

23 E. G. J. C. Warmerdam, A. M. C. H. van den Nieuwendijk, J. Brussee, A. van der Gen and C. G. Kruse, *Recl. Trav. Chim. Pays-Bas*, 1996, **115**, 20–24.

24 E. Moreno-Clavijo, A. T. Carmona, A. J. Moreno-Vargas, L. Molina and I. Robina, *Curr. Org. Synth.*, 2011, **8**, 102–133.

25 (a) Y. Bleriot, D. Gretzke, T. M. Krulle, T. D. Butters, R. A. Dwek, R. J. Nash, N. Asano and G. W. Fleet, *Carbohydr. Res.*, 2005, **340**, 2713–2718; (b) A. Bordier, P. Compain, O. R. Martin, K. Ikeda and N. Asano, *Tetrahedron: Asymmetry*, 2003, **14**, 47–51; (c) P. Jakobsen, J. M. Undbeck, M. Kristiansen, J. Breinholt, H. Demuth, J. Pawlas, M. P. Torres Candela, B. Andersen, N. Westergaard, K. Lundgren and N. Asano, *Bioorg. Med. Chem.*, 2001, **9**, 733–744; (d) J. Streith, A. Boiron, J.-L. Paillaud, E.-M. Rodriguez-Perez, C. Strehler, T. Tschauder and M. Zehnder, *Helv. Chim. Acta*, 1995, **78**, 61–72.

26 M. T. Moran, J. P. Schofield, A. R. Hayman, G. P. Shi, E. Young and T. M. Cox, *Blood*, 2000, **96**, 1969–1978.

27 L. I. Willems, J. Jiang, K.-Y. Li, M. D. Witte, W. W. Kallemeijn, T. J. N. Beenakker, S. P. Schröder, J. M. F. G. Aerts, G. A. van der Marel, J. D. C. Codée and H. S. Overkleef, *Chem.-Eur. J.*, 2014, **20**, 10864–10872.

28 A. Lammerts van Bueren, A. Ardèvol, J. Fayers-Kerr, B. Luo, Y. Zhang, M. Sollogoub, Y. Bleriot, C. Rovira and G. J. Davies, *J. Am. Chem. Soc.*, 2010, **132**, 1804–1806.

29 S. McNicholas, E. Potterton, K. S. Wilson and M. E. M. Noble, *Acta Crystallogr., Sect. D: Biol. Crystallogr.*, 2011, **67**, 386–394.

30 I. M. Aerts and S. van Weely, *Hum. Mutat.*, 1997, **10**, 348–358.

31 A. G. W. Leslie, *Acta Crystallogr., Sect. D: Biol. Crystallogr.*, 2006, **62**, 48–57.

32 W. Kabsch, *Acta Crystallogr., Sect. D: Biol. Crystallogr.*, 2010, **66**, 125–132.

33 P. Emsley, B. Lohkamp, W. G. Scott and K. Cowtan, *Acta Crystallogr., Sect. D: Biol. Crystallogr.*, 2010, **66**, 486–501.

34 G. N. Murshudov, P. Skubak, A. A. Lebedev, N. S. Pannu, R. A. Steiner, R. A. Nicholls, M. D. Winn, F. Long and A. A. Vagin, *Acta Crystallogr., Sect. D: Biol. Crystallogr.*, 2011, **67**, 355–367.

35 A. W. Schuttekkopf and D. M. F. van Aalten, *Acta Crystallogr., Sect. D: Biol. Crystallogr.*, 2004, **60**, 1355–1363.

36 A. A. Lebedev, P. Young, M. N. Isupov, O. V. Moroz, A. A. Vagin and G. N. Murshudov, *Acta Crystallogr., Sect. D: Biol. Crystallogr.*, 2012, **68**, 431–440.

